Industrial mould slags for continuous casting of stainless steel – analysis of the crystallisation behaviour using the Single Hot Thermocouple Technique

Marko Petajajarvi [1], Jeferson L. Klug [2,3], Paavo Hooli [1], Hans P. Heller [3], Piotr R. Scheller

1) Outokumpu Tornio Works, Finland

2) Federal University of Rio Grande do Sul, Brazil

3) Freiberg University of Mining and Technology, Germany

Abstract: During continuous casting the liquid slag infiltrates into the gap between the solidified strand and the mould generating a thin slag film. Due to the high temperature gradient the slag solidifies partially and remains partially liquid on the hot side. In the solid films taken in the tail-out phase at the end of the cast the cuspidine as the crystalline phase in the most part of the square section was detected. The crystalline phase in the slag film is formed partially during the solidification and partially via the devitrification process from solid phase and undergo changes with time. It is known that the solid film adhere at the mould wall with residence times of up to several hours. The crystallization of the solid layer affects the heat flux from the liquid steel into the mould cooling water and it affects the rate and uniformity of the steel shell solidification. The understanding and the control of the crystallization phenomena in the solid layer is important to be able to obtain desired cooling regime for different steel grades during a cast. In the collaborative work between Freiberg University of Mining and Technology, Germany, and Outokumpu Tornio Works, Finland, the crystallisation of complex industrial mould slags (CaO-SiO_2-Na_2O-Al_2O_3-Fe_2O_3-MgO-CaF_2(-MnO-K_2O-Li_2O-TiO_2)) used in the continuous casting of austenitic and ferritic stainless steels were investigated using the Single Hot Thermocouple Technique (SHTT) as well as heat flux measurement in the industrial process. With the SHTT technique time-temperature-transformation diagrams (TTT diagrams) were developed for various industrial slags, investigating the kinetics of crystallisation after quenching to different temperatures and isothermal holding. The solidification behaviour was observed *in situ* with cooling rates up to 3000 °C/min. In industrial experiments the local heat flux during casting was recorded with thermocouples installed in the mould wall. At the beginning of cast the liquid mould flux solidifies quickly against the mould wall forming a glassy solid layer. While casting the decrease of heat flux can be detected at the thermocouples and from mould cooling water. Recorded data from continuous casting machine is compared with the results achieved with the SHTT experiments.

Keywords: stainless steel; mould powders; hot thermocouple technique; continuous casting

1. Introduction

Outokumpu Stainless Oy at Tornio Works in Finland produces wide range of different steel grades with different properties in two melting shop lines and with two casting machines. The produced steel grades vary from relatively low chromium ferritic (EN 1.4003) to fully austenitic (EN 1.4310) steel grades. Also steel grades with high manganese content, ultra clean and steel grades with titanium/niobium stabilization are produced. The final products of Tornio Works are hot or cold rolled plates and strips from semi-finished products to high strength or high surface gloss products.

The wide range of different steel grades with different thermal and physical properties are challenging for continuous casting and for mould powders to ensure high productivity, stable casting process and high quality products. One of the key components to ensure high surface quality of slabs without defects in continuous casting is the control of solidification in mould. Depending on steel grade too high cooling rate in the mould can cause longitudinal cracks but with other steel grades too mild cooling can lead to bulging at secondary cooling zone and cause segregation, transverse and internal cracks. In Tornio Works at both casters the solidification rate in the mould is controlled with the properties of mould fluxes and their performance is followed with thermocouples installed in the mould and with total heat flux from liquid steel to mould cooling water.

The performance of mould powders is controlled by three physical and technological properties [1-4]: (i) viscosity (usually at 1300 °C), (ii) crystalline phase fraction developed in the slag film, and (iii) the thickness of both the liquid and solid layers of the slag film which are, in turn, dependent on the break (T_{br}) temperature of the mould slag.

Slag film samples were taken from the mould at the end of casting sequences [5, 6]. It was found that the most typical feature in the sampled films was the layer in which cuspidine crystals ($Ca_4Si_2O_7F_2$) were dominant. The films had a crystalline structure which either formed during cooling or via devitrification, i.e. crystallisation from the glassy state. It was observed that the residence time of the slag film or at least the part of the film in contact with the mould is very long – up to 10 hours or more.

Devitrification for mould slags is similar to that of ordinary glass [7]. Devitrification has an important role in continuous casting process, since it is related to surface roughness of slag films, which in turn can be related to interfacial thermal resistance and friction force at the mould/strand interface [6, 8, 9]. It was reported that friction in the continuous casting mould depends on the viscosity of mould slag and the type of crystalline phases present [10].

Glass formation and crystallisation are competitive processes. At room temperatures glasses can exist for extremely long periods of time because their high viscosity inhibits structural rearrangements required for crystal nucleation and growth. However, when a glass is heat-treated for a sufficiently long time at temperatures within or above the glass transition range, devitrification readily starts, as a rule, from the surface and sometimes in the bulk via heterogeneous or homogeneous nucleation [11, 12].

Although the mechanism of the heat transfer control by the crystallisation of cuspidine has not been determined yet, two ideas have been proposed. One is that radiation heat flux is decreased by scattering at the boundary between the crystalline and the liquid layers and the other is that total heat flux is decreased by the large thermal resistance of the air gap formed as a result of the solidification shrinkage. Anyway, cuspidine crystallisation from mould slag has the great effect on heat transfer control [13].

Once the mould powder is melted on the top of the liquid steel and the liquid flux infiltrates between the mould and the strand surface, the liquid slag is exposed to different cooling paths which can promote or prevent crystallisation. In fact it is common to see glassy parts of the slag in areas of high cooling rates with crystalline fractions at lower cooling rates. So, a proper characterization of the mould powder should include a complete description of the transformation kinetics.

TTT diagrams would unambiguously describe the crystallisation phenomena, providing a more fundamental understanding of the transformation process. Crystallisation for a commercial mould flux normally employed in the continuous casting of stainless steels was quantified with time-temperature-transformation (TTT) diagram using the Single Hot Thermocouple Technique, determining the beginning of crystallisation by direct observation [14]. It was reported that crystallisation in the industrial mould flux occurs by nucleation and growth of individual crystals in an undercooled liquid. The TTT diagram was divided into two separate regions, since two distinct C-shape curves were detected, suggesting two separate nucleation events, which would correspond to the precipitation of dicalcium silicate (Ca_2SiO_4) at temperatures over 1050 °C and of cuspidine ($Ca_4Si_2O_7F_2$) at temperatures below 1050 °C, according to X-ray diffraction from samples collected after the analysis. It was clearly observed that there is no specific crystallisation temperature for a mould flux but a range of temperatures defined by experimental conditions.

The Single Hot Thermocouple Technique (SHTT) can be used to build TTT diagrams. With this technique the sample is put on one thermocouple tip, heated and cooled at the desired rates. One feature of the technique is to allow *in situ* observation of melting and solidification under various thermal conditions. Due to the low mass of the system (sample and thermocouple) high heating and cooling rates (> 3000 °C/min) can be easily obtained. Besides SHTT, using the hot thermocouple technique another experimental mode is also possible: the Double Hot Thermocouple Technique (DHTT). With the DHTT the solidification behaviour can be observed in situ applying temperature gradients, simulating the conditions during continuous casting. In this mode the slag sample is placed between the tips of two thermocouples. Both sides can be controlled independently and mould-like temperature gradients or heat peaks can be applied [15].

In practise a common way to control the proportions of glass and crystals in the solid mould flux layer is by changing the basicity of the mould powder. The basicity of the mould powder gives a good estimation of the crystallization tendency but alone it often fails to describe the ability to control the heat flux in the mould. Construction of TTT diagrams for different mould fluxes used in practise gives more detailed information from the crystallization behaviour. Combining the information from TTT diagrams with the results collected from the casters can explain better their behaviour in the mould.

The development of the mould powders at melting shop is often done by trial and error method as all the factors related to their behaviour are not yet fully understood. The mould powder trials at the casting machine are time consuming and they always increase the risk for a breakout which can be very expensive. With better understanding of the behaviour of mould powders the amount of trials can be decreased at the casting machine thus the fine tuning of the mould powder properties can be made more accurately.

2. Experimental

2.1 Materials and samples preparation

The materials used at the measurements are industrial mould powders from different manufacturers used at the Outokumpu Stainless Oy Tornio Work's casting machines. The industrial mould powders composition as provided by the manufacturer can be seen in Table 1. Before measurements the mould powders were decarbonized in kiln furnace at

600°C for four hours. After decarbonisation the compositions of the mould powders were analysed with XRF and LECO CS244 (carbon). The compositions of the mould powders after decarbonisation are presented in table 2

Table 1. Composition and properties of the mould powders provided by supplier

Component	Powder A	Powder B	Powder C	Powder D
Basicity (CaO+MgO/SiO2)	1,08	1,09	1,17	1,00
CaO/SiO_2	1,05	1,06	1,17	-
SiO_2	34,9	31	30,9	30,9
CaO	-	-	36,1	29,5
MgO	-	-	-	1,5
CaO+MgO	37,63	34	-	-
Al_2O_3	6,34	6,25	7	7
Na_2O	-	-	7,3	8,4
K_2O	-	-	-	0,4
Na_2O+K_2O	6,71	8,25	-	-
MnO	0,05	3	-	3,9
Fe_2O_3	0,7	1,25	1,5	0,9
C_{free}	2,3	1,75	3	3
CO_2	6,5	7,25	4,8	6,7
C_{total}	4,05	4	-	4,8
F	6,35	7,25	7,5	9,1
H_2O (600°C)	0,71	0,8	-	0,2
Bulk density (kg/dm3)	0,64	0,63	0,88	
Softening point +/-30 (°C)	1040	980	1100	
Melting point +/-20 (°C)	1140	1070	1120	*1130**
Fluidity point +/-20 (°C)	1160	1080	1150	
Viscosity 1300°C (dPa*s)	2,8	1,1	1,2	0,99

**** Crystallization temperature (°C)***

Table 2. Analyzed compositions of the mould powders after decarburazation

Component	Powder A	Powder B	Powder C	Powder D
CaO	40,10	36,70	39,01	33,84
SiO_2	38,02	33,97	35,04	33,56
Fe_2O_3	0,64	1,30	1,75	1,94
MgO	0,84	1,29	0,88	1,47
Al_2O_3	6,65	6,78	7,66	7,47
MnO	0,01	3,12	0,03	3,53
K_2O	0,01	0,07	0,45	0,42
P_2O_5	0,07	0,06	0,23	0,86
Na_2O	6,75	8,73	7,82	9,67
TiO_2	0,28	0,28	0,13	0,41
F	5,78	7,36	6,40	6,71
C	0,85	0,36	0,60	0,12
Tot.	100,00	100,00	100,00	100,00

2.2. The Hot Thermocouple Technique

The apparatus used in the present work was constructed in the Institute of Iron and Steel Technology of the Freiberg University of Mining and Technology, Germany [15]. A schematic view is given at Figure 1. It consists basically of two systems: an observation system and a thermocouple system. In a vacuum chamber there are two water-cooled inserts left and right. Both of them hold a B-type thermocouple at tips. Each thermocouple is connected to a separate thermocouple controller. The material under study is melted directly on thermocouple inside the vaccum chamber. The thermocouples remains inside an additional heating, i.e. a kanthal coil which reduces heat losses from the sample to the surroundings.

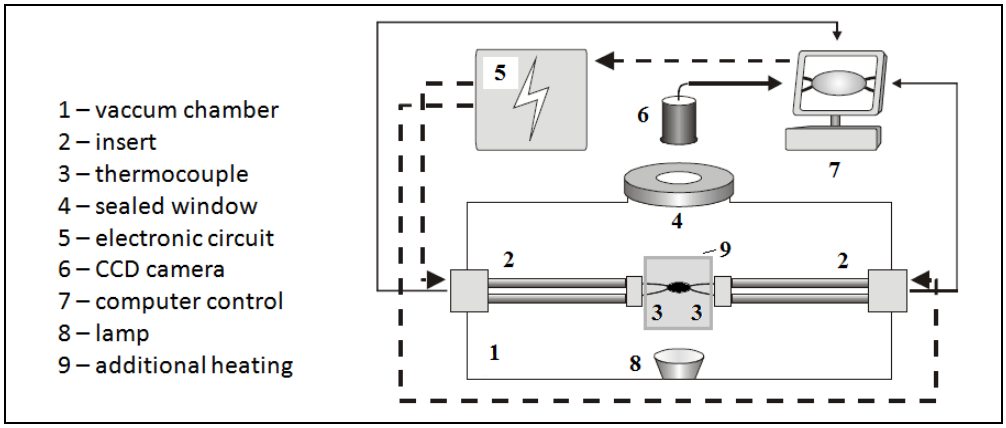

Figure 1. Schematic view of the experimental set-up used in the present work.

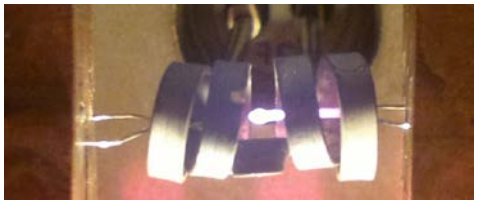

Figure 2. Industrial mould flux sample completely melted at 1400 °C on the thermocouple tip in the additional heating coil.

With this experimental set-up it is possible to measure the sample temperature with a thermocouple while it is heated simultaneously. A computer manages the two thermocouple controllers, controlling individually heating and cooling conditions. Software superimposes information about time, temperature and sample image into videos files in a real-time system. More details on calibration of the apparatus can be found in other publication [16].

2.3 Experimental procedure

To execute the experiments small portions of mould powders samples (typically 4.5-6 mg) are pressed and put on the thermocouple tip. With the substances in the vacuum chamber it is applied 10 min of vacuum with 10 mbar. Then, the vessel is filled with Ar, maintaining a flux of 300 l/h during the measurements. The additional heating is turned on, maintaining ca. 500 °C around the thermocouple. The slag samples are heated and melted directly on the thermocouple tip, using one thermocouple per slag. During the operation lime slurry is maintained at the gas exit. The experiments are registered with video files.

In the present work time-temperature-transformation (TTT) diagrams were built applying very high cooling rates (higher than 3000 °C/min) as illustrated at Figure 3. From this point the incubation time is measured by direct observation.

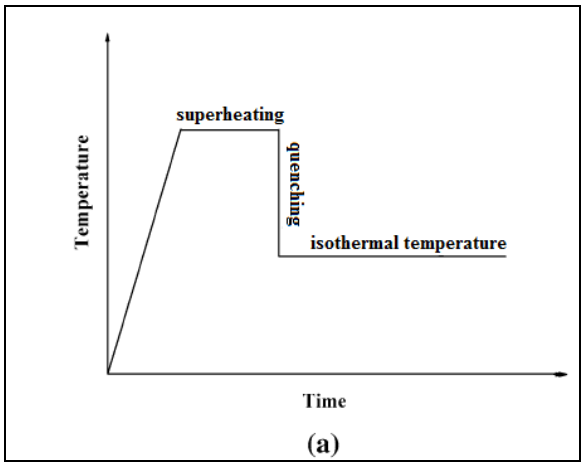

Figure 3. Typical thermal profile to get data for TTT diagrams.

The measurement procedure was chosen based on preliminary measurement to hold the sample in place during the melting and to stabilize bubble formation during melting. The heating of the sample from ambient temperature was made with heating rate of 100°C/min up to 1400°C, where the sample was kept for 60 seconds before quenching to a chosen incubation temperature as fast as possible (approx. 3000 °C/min). After detection of first crystals the sample was heated up to 1400°C as fast as possible and kept there for 60 seconds before quenching again to same incubation temperature as before. If no crystals were detected after ~1500 seconds the sample was heated up again. For each measured temperature the quenching and incubation was repeated six times with the same sample. For each measured temperature a new sample was used.

After the measurement the result were viewed from video file saved during the measurement. The incubation times required to form first crystals were determined from the video. If no crystals were detected a value of 10 000 seconds was recorded to the results. In some measurements the video clearly revealed that the sample was not completely melted before first quenching and resulted instant crystallization of the sample. To make the results more comparable between different mould fluxes the first incubation times were discarded from the final results with all mould fluxes.

Repeating the quenching to same temperature several times and using a new sample for each temperature eliminates the effect of volatile components of e.g. F and Na to the TTT diagram. At the same time the repeated measurements gave information how the volatilization of the components during the measurement effect to the incubation time. The problem with this technique is increasing scattering of the results at each temperature and the amount of volatilization at initial heating and during the measurements is unknown.

3. Results

3.1 TTT diagrams for mould fluxes A, B, C and D

The TTT diagrams for the mould fluxes A, B, C and D constructed with SHTT measurements are presented in Figures 4, 5, 6 and 7 respectively.

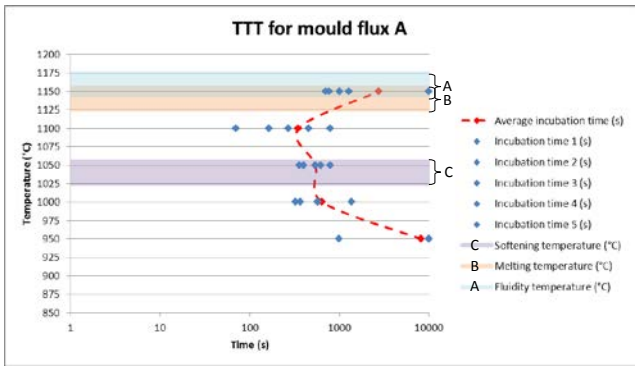

Figure 4. TTT diagram for the mould flux A

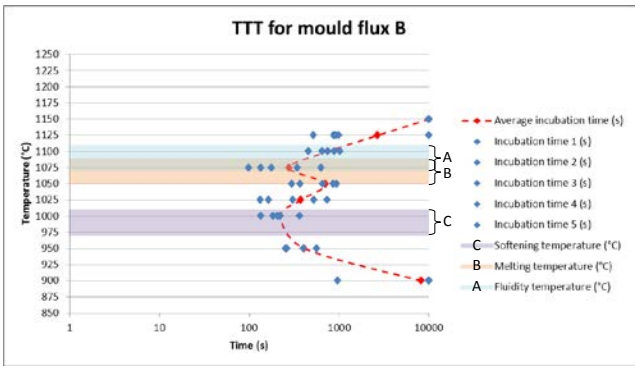

Figure 5. TTT diagram for the mould flux B

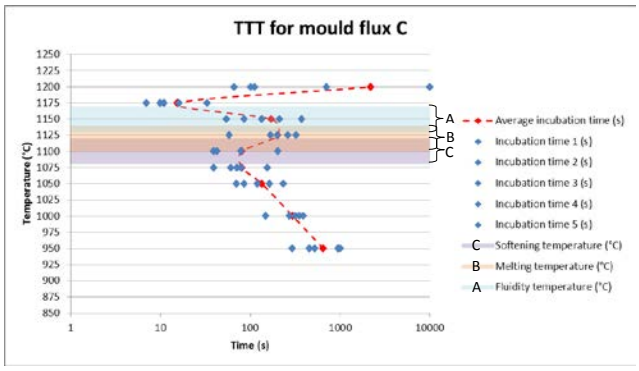

Figure 6. TTT diagram for the mould flux C

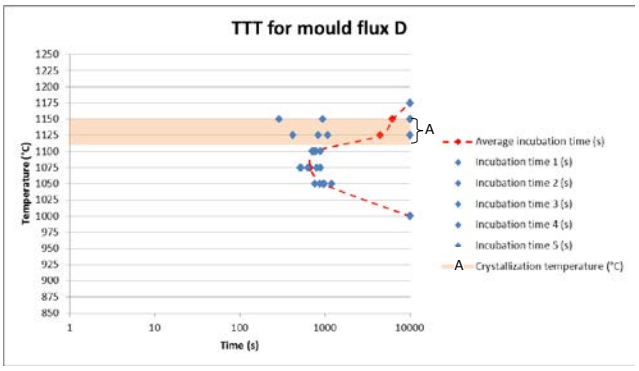

Figure 7. TTT diagram for the mould flux D

The construction of the TTT diagram for the mould flux A was the most difficult one as the repeatability of the results was poor compared to the other measured mould fluxes, since the scatter is high. In the Figure 4 the results from the samples where incubation times were shortest at are presented. Due the poor repeatability of the measurements with the mould flux A the conclusions made from the TTT diagram for this mould flux have to be made with some consideration.

3.2 Comparison of the TTT diagrams

In the Figure 8 is presented the average values of individual TTT diagrams in Figures 4, 5, 6 and 7 in one graph and it shows the differences in crystallization tendency between the different mould fluxes A, B, C and D. Based on the incubation times the mould flux C has the highest tendency to crystallize at temperatures above 1025 °C. It also has the widest measured temperature rage (between 950 – 1200 °C) where the crystals are formed. On the opposed side is the mould flux D, which had the longest incubation times and shortest temperature rage. The mould fluxes A and B behaved similarly as regarding the crystallization behaviour and temperature range. The main difference between fluxes A and B is the mould flux B's tendency to form crystals at lower temperatures. At temperatures below 1025 °C the crystallization of mould flux B is fastest. With the mould fluxes A, B and C the two C-shaped curves can been seen at the TTT diagram. Based on previous research the two C's are an indication of formation of two different types of crystals. With the mould flux D only one C can be observed at the TTT diagram with average incubation times but the Figure 7 shows scattering in the results at temperatures above 1100 °C and the presence of second C cannot be

completely ruled out.

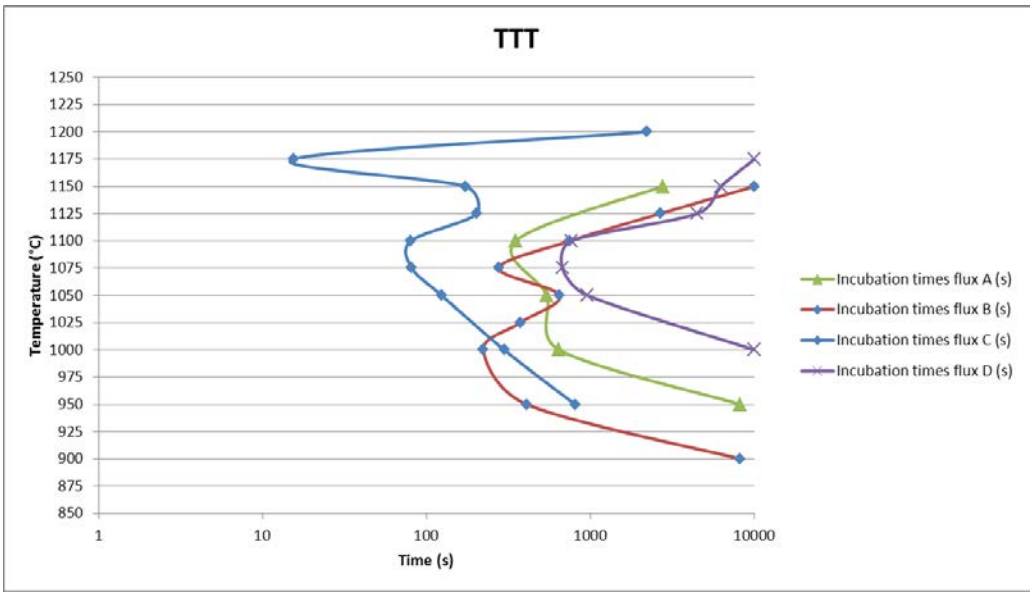

Figure 8. Combined TTT diagrams of mould fluxes A, B, C and D

4. Discussion

The crystallization behaviour of the mould fluxes measured with the SHTT correlate with basicity which was expected. The TTT diagrams and the basicity suggests that the mould flux C is the most mild cooling mould flux compared to other measured fluxes. Anyhow at the casting machine these relations change and crystallization tendency of the mould flux doesn't alone explain the heat transfer properties of the solid mould flux layer. In several studies it is mentioned that there are other properties e.g. viscosity and break temperatures [1] and based on the results from the caster these properties need to be considered more carefully.

4.1 Comparison between mould fluxes A and C

Most of the ferritic steel grades in Outokumpu Tornio Works are casted at the caster no. 1 (CC1) where mould powders A and C have been used to cast steel grade EN 1.4016, which is basic ferritic stainless steel without Ti, Nb or Al. EN 1.4016 is good steel grade for comparing of the behaviour of the mould powders as the amount of inclusions absorbed from the steel is small and the composition of the mould flux stays relatively stable through the whole cast. In the Figure 9 is presented average values of total heat flux values per surface area of the mould for several slabs. In total the data consists of information from 697 slabs (approx. 170 heats). The x-axis in the Figure 9 is casting speed (m/min) times steel temperature in tundish (°C) to give an impression from the amount of heat flow in to the mould. The value doesn't describe exact the amount of energy flowing in to the mould but it makes the values more comparable between casts made with different casting speeds and superheats. From the Figure 9 can be seen that the heat flux from the liquid steel to mould cooling water is higher with the mould flux C than with the mould flux A. The behaviour between mould fluxes A and C is opposite what the crystallization behaviour in the TTT diagram suggests as the higher crystallization tendency of mould flux C should inhibit the heat flux more with the mould flux A.

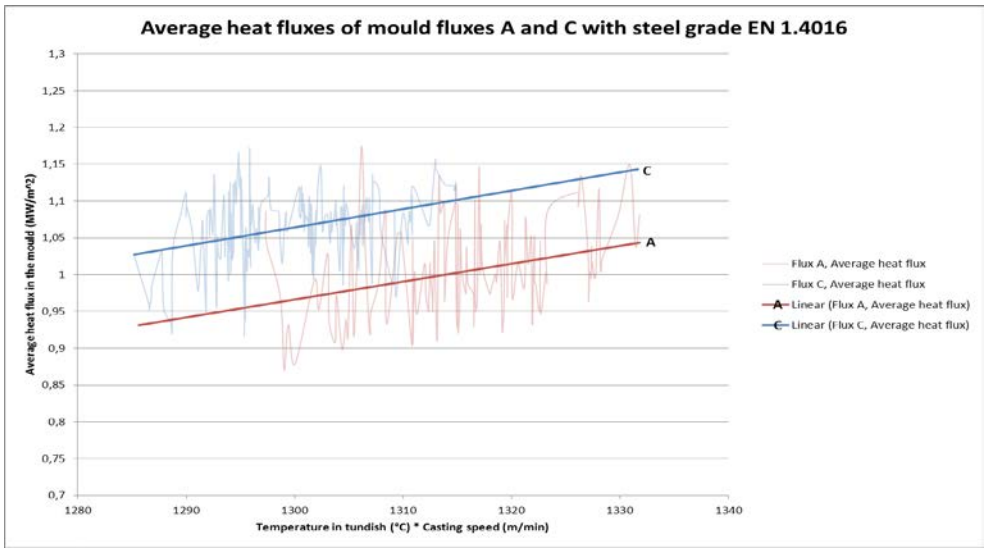

Figure 9. Average heat fluxes for EN 1.4016 slabs casted with mould powders A and C

A similar relation between behaviour of the mould fluxes A and C was also observed at the Outokumpu Tornio Works caster no.2 (CC2) when casting EN 1.4016 steel grade. The cast of three heats was started with mould powder A and after the dummy bar was out of the machine the mould level started to show signs from unsteady bulging of the strand. The casting speed was decreased in order to control the bulging but the amplitude of mould level variation kept increasing. When the casting of the second heat was started and the bulging was getting severe the mould powder was changed to mould powder C during the casting. Shortly after the mould powder change the bulging started to level out and the mould level variation amplitude begun to decrease. Before the second ladle was empty the mould level variation had decreased to normal level and the mould level variation frequency did not show indications from bulging. The rest of the cast was done with the mould powder C and during the third heat the casting speed was increased to normal. In the Figure 10 is presented the mould level and stopper rod behaviour when of the bulging cast. The time of the mould powder change is marked in the graph with red dashed line.

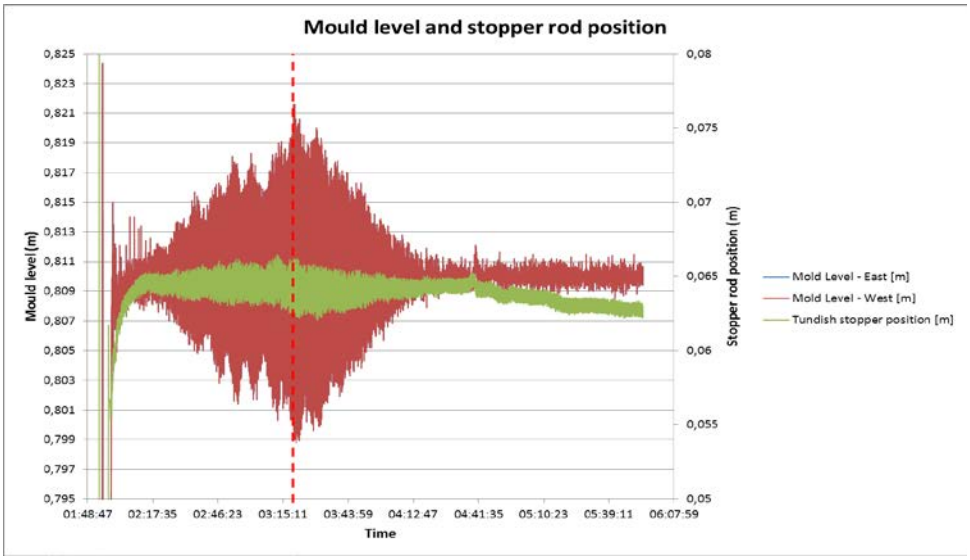

Figure 10. Mould level and stopper rod behaviour in a cast of unsteady bulging

Interesting phenomena in the bulging cast was that the temperatures recorded from the thermocouples installed in to the mould or the heat flux values from mould cooling water did not show significant changes in their values after the mould powder change. The only indication from stronger cooling with the mould flux C was the disappearance of the bulging which is sign from formation of thicker and stronger steel shell in the mould.

4.2 Comparison between mould fluxes A and D

Also the mould powder D has been used at the CC1 in Tornio to cast ferritic steel grade EN 1.4016 and the heat flux values of the mould fluxes A and D are presented in the Figure 11. The amount of available data for the mould flux D was less than for mould flux A or C and the average heat flux values for mould flux D were calculated in 0,5 m intervals. The heat flux values for the mould flux D are located more on the right in the Figure as casting speed were slightly higher than in the more accurate comparison data collected for the mould flux A. Based on the TTT diagram of the mould flux D it is the most high cooling mould flux with the lowest tendency to from crystals. Mould powder D also has the lowest basicity. Between mould fluxes A and D the heat flux measurement results agree with the result obtained from the SHTT measurements.

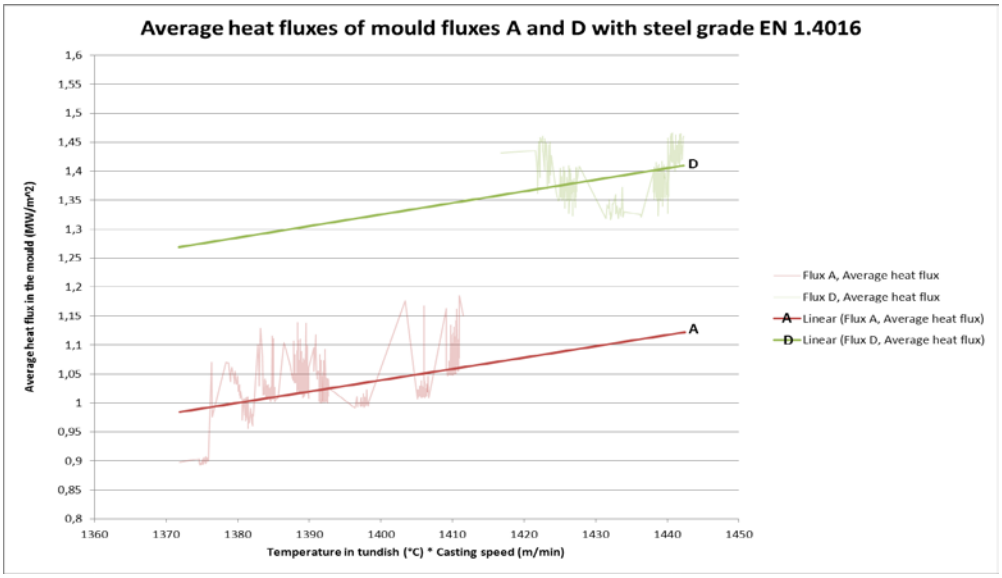

Figure 11. Average heat fluxes for EN 1.4016 0,5 m sections casted with mould powders A and D

4.3 Mould flux B

The crystallization tendency of mould flux B in the TTT diagram settles between the mould fluxes A and C and can be described as medium cooling mould flux. The mould powder B is used in Outokumpu Tornio Works to cast several different steel grades but because of lack of comparison data with other mould powders from casters its behaviour cannot be discussed with more details.

4.4 Break temperature and viscosity of the mould fluxes

In the table 3 is presented characteristic calculated values for the mould powders A, B, C and D from the analysed chemical compositions after decarburisation. Some of the values differ (e.g. viscosity) from the values reported by the supplier and they are also reported in the table in square brackets. When comparing the values for mould powders A and

C two values can be found, which can explain the higher heat resistance with the mould flux A than mould flux C. The higher viscosity and break temperature of the mould flux C suggests that it forms thicker solid layer between the mould wall and steel shell which would cause even higher resistance to thermal transfer than the quickly crystallizing mould flux C. The break temperature of the mould flux D is the lowest leading to thin solid layer and low thermal resistance. The values in the table 3 and observations made at the caster suggest that regarding the heat transfer properties of the solid layer in the mould the viscosity and break temperature of mould fluxes are more dominating factors than the basicity and crystallization tendency of the mould flux.

Table 3. Calculated properties of the mould fluxes

Component	Flux A	Flux B	Flux C	Flux D
Basicity (CaO/SiO2)	1,05	1,08	1,11	1,01
Basicity (CaO+MgO/SiO2+Al2O3)	0,92	0,93	0,93	0,86
Viscosity IRSID [manufacturer] (dPa*s at 1300 °C)	3,6 [2,8]	1,5 [1,1]	2,4 [1,2]	1,8 [0,99]
Break temperature (°C)	1203	1141	1165	1096
NBO/T	2,86	3,47	3,10	3,27

5. Conclusions

Crystallization behaviour of four different industrial mould powers use in Outokumpu Tornio Works were studied in Freiberg University of Mining and Technology with SHTT to construct their TTT diagrams. The results obtained from SHTT were compared to observations and measurement result from the two continuous casting machines. Between two mould fluxes a contradiction between the TTT results and the behaviour in the continuous casting machine was observed as the flux with highest tendency to crystallize did not have the lowest thermal conductivity during casting. The contradiction in their behaviour can be explained with the differences in viscosity and break temperature but at the same time the explanation leads to a conclusion that considering the thermal properties of the solid mould flux layer in the mould the viscosity and break temperature are dominating factors over the basicity and crystallization tendency.

Acknowledgements

The author Marko Petäjäjärvi wishes to express his gratitude to FIMECC Oy (Finnish Metals and Engineering Competence Cluster) from funding the MOCASTRO-project and making possible the researcher exchange to Freiberg University of Mining and Technology. The author wishes also to grant huge “Thank you” to all the personnel working and studying in Freiberg University of Mining and Technology from all the received help and warm welcome.

References

1. Mills, K.C. and A.B. Fox, *The role of mould fluxes in continuous casting - so simple yet so complex.* ISIJ International, 2003. **43**(10): p. 1479-1486.
2. Branion, R.V., *Mold fluxes for continuous casting.* Iron and Steelmaker, 1986(September).
3. Pinheiro, C.A., I.V. Samarasekera, and J.K. Brimacombe, *Mold flux for continuous casting of steel, Part III.* Iron and Steelmaker, 1994(December).
4. Sridhar, S., Mills, K.C., Afrange, O.D.C., Lorz H.P., Carli R., *Break temperatures of mould fluxes and their relevance to continuous casting.* Ironmaking and Steelmaking, 2000. **27**(3): p. 238-242.

5. Hooli, P., *Study on the layers in the film originating from the casting powder between steel shell and mould and associated phenomena in continuous casting of stainless steel*. 2007, PhD dissertation, Helsinki University of Technology.
6. Kromhout, J.A., *Mould powders for high speed continuous casting of steel*. 2011, PhD dissertation, Technische Universiteit Delft.
7. Mizuno, H., Esaka, H., Shinozuka, K., Tamura, M., *Analysis of the crystallization of mold flux for continuous casting of steel.* ISIJ International, 2008. **48**(3): p. 277-285.
8. Li, Z., Thackray, R., Mills, K. C., *A test to determine crystallinity of mould fluxes*, in *VII International Conference on Molten Slags, Fluxes and Salts*. 2004: Cape Town, South Africa. p. 813-819.
9. Carli, R. and C. Righi, *Mould flux crystallization: a kinetic study*, in *VII International Conference on Molten Slags, Fluxes and Salts*. 2004: Cape Town, South Africa.
10. Hering, L., H.P. Heller, and H.W. Fenzke, *Untersuchungen zur Giesspulverauswahl beim Brammenstranggiessen (German).* Stahl und Eisen, 1992. **112**(8): p. 61-65.
11. Zanotto, E.D., *Crystallization of liquids and glasses.* Brazilian Journal of Physics, 1992. **22**(2).
12. Fokin, V.M., Zanotto, E. D., Yuritsyn, N. S., Schmelzer, J. W. P., *Review - homogeneous crystal nucleation in silicate glasses: a 40 years perspective.* Journal of Non-Crystalline Solids, 2006. **352**: p. 2681-2714.
13. Nakada, H. and K. Nagata, *Crystallization of CaO–SiO_2–TiO_2 slag as a candidate for fluorine free mold flux.* ISIJ International, 2006. **46**(3): p. 441-449.
14. Kashiwaya, Y., C.E. Cicutti, and A.W. Cramb, *An investigation of the crystallization of a continuous casting mold slag using the Single Hot Thermocouple Technique.* ISIJ International, 1998. **38**(4): p. 357-365.
15. Lachmann, S. and P.R. Scheller, *Effect of Al_2O_3 and CaF_2 on the solidification of mould slags and the heat transfer through slag films*, in *VIII International Conference on Molten Slags, Fluxes and Salts*. 2009: Santiago, pp. 1101.
16. Klug, J.L., Hagemann, R., Heck, N. C., Vilela, A. C. F., Heller, H. P., Scheller, P. R., *Study of the solidification behaviour of metallurgical slags using the Single Hot Thermocouple Technique*, in *IX International Conference on Molten Slags, Fluxes and Salts*. 2012: Beijing, China.
17. Prapakorn, K. and A.W. Cramb, *Initial solidification behavior in continuous casting: the effect of MgO on the solidification behavior of CaO-Al_2O_3 based slags*, in *MS&T Conference Proceedings*. 2004.
18. Orrling, C., Cramb, A. W., Tilliander, A., Kashiwaya, Y., *Observations of the melting and solidification behavior of mold slags.* I&SM, 2000(January).
19. Orrling, C. and A.W. Cramb, The effect of water vapor on mold slag crystallization. Metallurgical and Materials Transactions B, 2000. **31B**(April).